Journal of Applied Polymer Science

# Calcium Alginate Fibers Containing Metallic Nanoadditives

**Maciej Boguń,[1] Grzegorz Szparaga,[1] Paulina Król,[1] Teresa Mikołajczyk,[1] Stanisław Rabiej[2]**
[1]Departament of Material and Commodity Sciences and Textile Metrology, Lodz University of Technology, 90-924, Lodz, Poland
[2]Department of Physics and Structural Research, University of Bielsko-Biala, 43-309, Bielsko-Biała, Poland
Correspondence to: M. Boguń (E - mail: maciek.bogun@wp.pl)

**ABSTRACT:** In this manuscript two types of nanocomposite alginate fibers containing metallic nanoadditives: silver or $Fe_3O_4$ were obtained. The effect of the process parameters and the influence of the amount of nanoadditives in the fibers matrix on the mechanical properties, crystalline structure, porous structure, and sorption properties was investigated. The resulting fibers are characterized by the level of tenacity up to 23 cN/tex, the degree of crystallinity about 30%, and high sorption properties, which are strictly connected with hydrophilic nature of the polymer. On the basis of the images obtained by using an electron microscope linked to an X-ray microanalysis it was found that the distribution of nanoadditives in the material of calcium alginate fibers is uniform. © 2013 Wiley Periodicals, Inc. J. Appl. Polym. Sci. **2014**, *131*, 40223.

**KEYWORDS:** biodegradable; biomaterials; nanoparticles; nanowires and nanocrystals; fibers

Received 12 August 2013; accepted 23 November 2013
**DOI: 10.1002/app.40223**

## INTRODUCTION

The directions being taken in the development of alginate fibers are linked to their increasingly numerous medical applications.[1] Such properties as specific ability to accelerate the wound healing process, chondrogenic action, high sorption, and easy gelification mean that such fibers are widely used to make dressing materials.[2–5] The gelification process is dependent on the material of the fibers, and particularly its chemical structure.[6,7] Gelification takes place more easily in the case of fibers made from a polymer where the majority of blocks are derived from mannuronic acid. This makes it possible for the dressing to be matched to the appropriate stage of wound healing. The same effect can also be obtained using fibers made from types of alginate other than calcium alginate. For healing infected wounds and wounds at a later stage of healing dressings, materials made from zinc alginate fibers are the most appropriate. The new-generation fibers made from alginic acid, combined with antibiotic, provide possibilities for the local treatment of heavily infected wounds without the need for frequent replacement of the dressing,[8] because such fibers enable the gradual release of the antibiotic into the environment of the wound.

Fibers made of copper alginate (as has been confirmed by us), when in contact with the skin, show the ability to generate a negative static electrical charge.[9] This has a favorable effect on the surroundings of the wound, causing a reduction in the pain experienced by patients. Dressings made of such fibers can be used on skin lesions without exudate, e.g., bedsores or wounds at the granulation tissue growth stage. Fabrics made of copper alginate can also be used to make hospital linen and various types of folding mattresses.

The further development of alginate fibers is linked to the use of nanotechnology in the process of their manufacture. This makes it possible to give them entirely new properties not previously found in traditional fibers. It also extends their range of use. Calcium alginate fibers containing various types of ceramic nanoadditives can be used to make a new generation of composite materials useful for bone tissue regeneration.[10] The presence in the fibers of such nanoadditives as HAp, TCP, bioglass, and $SiO_2$ has the effect of supporting the process of bone tissue reconstruction. The specific structure of a composite material with diverse porosity gives it the properties of a modern implant material. Its construction, the principle of its action, and its properties were described in Refs. 11–14. The ways in which the presence of various types of ceramic nanoadditives in the calcium alginate fiber material, and the basic parameters of the production process, affect the structure and properties of the fibers have been the subject of analysis in a series of research works.[12,13,15,16]

Dressings can also be adjusted to the type of wound and stage of healing by means of the appropriate choice of components of the hybrid nonwoven fabric dressing. Calcium alginate fibers containing nanosilver, which was studied in the present investigation, are expected to serve as one of the components of such a new-generation dressing material. The presence of silver

nanoadditive in the fiber material will increase the antibacterial activity of the dressing as a whole.[17–19] Meanwhile, calcium alginate fibers containing the nanoadditive $Fe_3O_4$ are expected to be used as a component of a hybrid implant material for bone tissue regeneration. Such an implant material containing fibers with $Fe_3O_4$ nanoadditive in addition to ingredients supporting the tissue regeneration will make possible the imaging of the implant after it is fitted, using medical imaging methods. It will therefore be possible to monitor its resorption into the body, which is important in complex reconstructions of bone tissue defects.

The purpose of this work was to make a comparative analysis of the effect of the quantity of two different nanoadditives—silver and $Fe_3O_4$—introduced into the material of calcium alginate fibers, on the macroscopic and supramolecular structure of the fibers and their sorption and strength properties.

It was assumed that, as in the case of ceramic nanoadditives, the presence of metallic nanoadditives would lead to a change in the deformability of the fibers in the successive processes involved in their production. The course of these processes in turn affects the structure and final properties of the fibers. In the case of ceramic nanoadditives it was found[12,13] that the deformability was reduced, and this was accompanied by a reduction in strength properties when compared with fibers without nanoadditive. Having regard to the easier processing of the alginate fibers into nonwoven fabric, and their particular intended use, it was attempted in this work to obtain fibers whose specific strength values were as high as possible. As well as the quantity of nanoadditive, factors strongly affecting the properties and structural parameters of the fibers also include a basic parameter of the forming process—the as-spun draw ratio—and the associated attainable deformation at both stages of plasticization drawing. The as-spun draw ratio was varied over a wide range of positive values, from 35 to 120%, the use of positive values of this parameter being favorable when making alginate fibers with a rigid macromolecular structure.[12,13] Other parameters of the fiber forming process, such as the composition and temperature of the solidification and plasticization baths, were determined on the basis of preliminary tests.

## EXPERIMENTAL

### Materials

Calcium alginate fibers containing metallic nanoadditive of silver or $Fe_3O_4$ were made using sodium alginate polymer with the trade name Protanal LF 10/60LS (FMC Biopolymer, Norway). This polymer was characterized by the increased amount of mannuronic acid to guluronic acid, commonly known as high-mannuronic sodium alginate. The high-mannuronic sodium alginate has macromolecules with the majority of blocks derived from $\beta$-mannuronic acid (between 55 and 65% of the blocks, according to the manufacturer). The substance has been tested negative for bacterial content. The average molecular mass $M_w$ determined by gel chromatography (SEc/GPC) was 1,096,772 g/mol. The polydispersity index calculated based on the ratio $M_w/M_n$ was 7.1. The polymer also had a fairly wide molecular mass distribution curve.

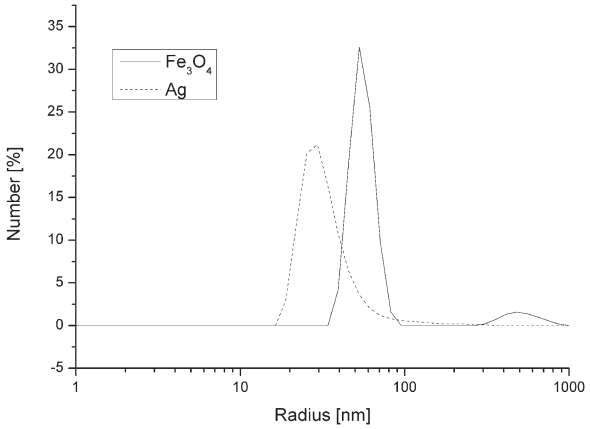


**Figure 1.** Grain size contributions for the silver and $Fe_3O_4$ nanoadditives by number.

Two metallic nanoadditives were used: silver and $Fe_3O_4$. The nanosilver was a commercial product from Sigma-Aldrich, with grain sizes (according to the manufacturer) of below 100 nm. The $Fe_3O_4$ nanoadditive was also a commercial product from Sigma-Aldrich, with grain sizes (according to the manufacturer) of below 50 nm.

The particle size distribution of the nanoadditives was analyzed by dynamic laser light scattering (DLS) using a Zetasizer instrument (Malvern Instruments). The samples were prepared as a dispersion with 0.01% concentration of tested material in water. Before measurement those dispersion were treated with ultrasonic probe for 1 h in temperature approximately about 40°C. DLS measurement was taken in temperature 25°C. It was found that the particle sizes of the silver nanoadditive are in the range 18–307 nm, with a maximum peak at 29 nm (Figure 1). For the $Fe_3O_4$ nanoadditive two peaks were recorded, at 39–82 nm and 307–859 nm, with the first peak corresponding to ~93% of the amount of the sample. The maximum for this peak was at ~53 nm (Figure 1). SEM images of the nanoadditives are shown in Figure 2.

### Fiber Formation

The fibers were formed by wet spinning from aqueous solutions of sodium alginate with a concentration of 7.4%. The design of the spinning machine enabled the stabilization of the technological parameters at a desired level, and constant monitoring of those parameters. The drawing systems used enabled continuous adjustment of the linear speed over a range from 0.5 to 33 m/min. The degree of draw was monitored by continuous measurement of the rotational speed using a digital frequency meter. After deaeration, the spinning solution was supplied under the pressure to a gear pump with a capacity of 0.6 $cm^3$/rev. The fibers were formed using a 500-hole nozzle with a hole diameter of 0.08 mm. The average flow speed of the spinning liquid in a channel of the spinning nozzle was 2.09 m/min.

The fiber solidification process was carried out in a bath with a 3% content of $CaCl_2$, at a temperature of 20°C and a pH of 3.1–3.6. The drawing process took place in two stages: the first was in a plasticization bath with the same composition as the coagulation bath, but with its temperature raised to 70°C; the

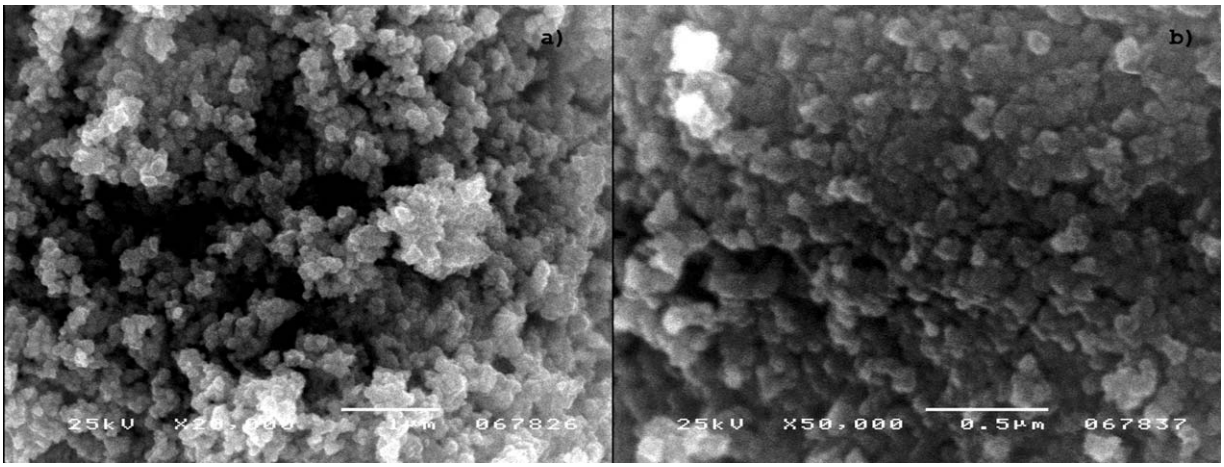


**Figure 2.** Images of the nanoadditives used: (a) nanosilver and (b) $Fe_3O_4$.

second stage took place in superheated steam at 135°C. After the spinning process the fibers were rinsed and dried in isometric conditions.

**Testing Methods**

The rheological characteristics of the spinning solutions were determined using an Anton Paar Rheolab QC rotary rheometer. Measurements were performed for shear rates ranging from 0.2 to 100 $s^{-1}$ and shear stresses ranging from 12 to 1200 $N/m^2$, at 20°C. The rheological characteristics of spinning solutions containing different quantities of the two nanoadditives were evaluated based on the values determined for the rheological parameters $n$ and $k$ in the Ostwald–de Waele equation.

The macroscopic structure of the fibers was investigated using a scanning electron microscope (SEM JSM 5400 JEOL).

The porous structure was investigated by mercury porosimetry using a Pascal 440 porosimeter (CE Instruments). It was assumed that the total volume of pores in the range 3–7500 nm determined in the fibrous material included both the porosity of the fibers themselves (in a range up to 1000 nm), and the porosity resulting from defects in the structure of the fiber surface and spaces between monofilaments (in a range above 1000 nm).

The distribution of the nanoadditives in the fibers was analyzed using EDX spectra produced using a scanning electron microscope (ISM5400) with an analyzer of characteristic X-ray energy dispersion (EDS LINK JSIS, from Oxford Instruments).

Tests of the supramolecular structure of calcium alginate fibers with silver and $Fe_3O_4$ nanoadditives were performed by the X-ray diffraction method (WAXS) using a URD 6 diffractometer (Seifert, Germany) with a copper lamp emitting radiation of wavelength $\lambda = 1.54$ Å with power supply parameters $U = 40$ kV and $I = 30$ mA. The radiation was monochromatized using a graphite monochromator. The diffraction curves were recorded using a reflection method and stepwise measurements over an angular range $2° = 3°$ to 60° with a step size of 0.1°. The tested fibers was powdered using a microtome to eliminate texture, and then pressed into tablets with a diameter of ~2 cm and a thickness of 1 mm.

The sorption properties of the fibers at 65% RH and 100% RH were determined in accordance with the Polish standard PN-P-04601:1991.

Water retention was measured by comparing the mass of water remaining in the fibers after centrifuging at an acceleration of 10 000 $m/s^2$, to the mass of the completely dried-out fibers.

The specific strength of the fibers was determined using an Instron tensile testing instrument, in accordance with the PN-EN ISO5079:1999 standard.

## RESULTS AND DISCUSSION

**Evaluation of the Rheological Properties of the Spinning Solutions**

The rheological properties of spinning solutions determine the proper processing of those solutions into fibers, the stability of the forming process, and the absence of tearing of elementary fibers at the spinning nozzle. Tearing of elementary fibers may be caused by crumbling or by capillary disintegration resulting from incorrect choice of apparent dynamic viscosity. The behavior of solutions may also be affected by the presence of variable quantities of metallic nanoadditives. Such an effect on the rheological properties of liquids was found in the case of ceramic nanoadditives.[20]

Analysis of the flow curves, of which examples are shown for 1% content of silver and $Fe_3O_4$ nanoadditives (Figure 3), shows that these are shear thinning non-Newtonian fluids without flow boundary, as the tangential stress increases less than proportionally to the increase in the shear rate, while the curves pass through the origin of the coordinate system. The character of the curves is maintained regardless of the quantity of either type of nanoadditive. There is a small change in the values of the rheological parameters $n$ and $k$ (Table I).

Changes in the apparent dynamic viscosity as a function of the shear rate for solution with 1% content of each type of nanoadditive are illustrated in Figure 3. Those solutions follow a pattern typical of polymer solutions. The apparent dynamic viscosity decreases as the shear rate increases.

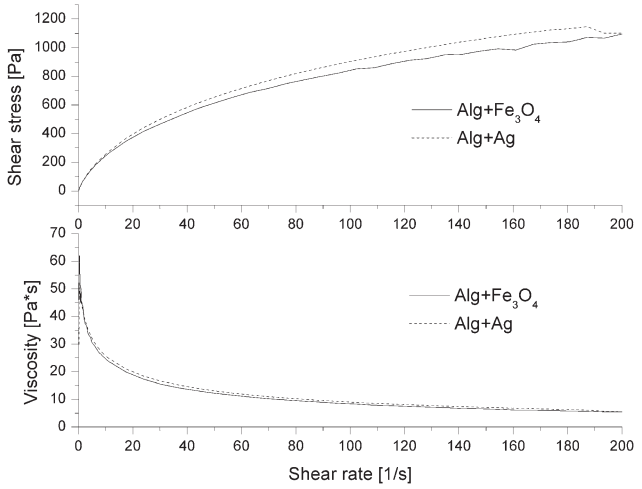


**Figure 3.** Flow curves and dependence of apparent dynamic viscosity on shear rate for sodium alginate solutions containing 1% nanosilver or nano $Fe_3O_4$

The tested solutions show good stability of rheological parameters 24 h after their preparation, but after 7 days there is observed to be an increase in the parameter *n* and a decrease in the parameter *k*.

It should also be noted that changes in the quantity of nanoadditive in the range 1–3% do not cause significant changes in the values of the rheological parameters *n* and *k*.

### Analysis of Strength Properties of Nanocomposite Alginate Fibers with Regard to Their Supramolecular Structure

The wet spinning method of fiber formation was conducted in a several steps process. All stages: solidification and the subsequent drawing stages were carried out in defined and constant conditions like: composition, media, and temperature. The only variable parameter was as-spun draw ratio. During the formation of fibers containing different quantities of both nanosilver and $Fe_3O_4$ as nanoadditives, the value of the as-spun draw ratio was varied over a range of positive values.

**Table I.** Rheological Properties of Spinning Solutions Containing Different Quantities of Silver and $Fe_3O_4$ Nanoadditives

| Type and quantities of nanoadditives | Rheological parameters | |
|---|---|---|
| | "*n*" | "*k*" |
| 1% $Fe_3O_4$ | 0.674 | 47.93 |
| 2% $Fe_3O_4$ | 0.705 | 46.71 |
| 3% $Fe_3O_4$ | 0.694 | 48.79 |
| 1% Ag | 0.711 | 45.58 |
| 2% Ag | 0.720 | 43.50 |
| 3% Ag | 0.700 | 48.67 |
| Without nanoadditives | 0.637 | 42.86 |

Analysis of the effect of the as-spun draw ratio on the deformability at the drawing stage and the strength properties of fibers containing nanosilver (Figure 4) shows that a change in this parameter towards larger positive values, irrespective of the quantity of nanoadditive used, leads to a reduction in deformability, and consequently lower values of total draw ($R_c$). For a 1% content of nanosilver, $R_c$ is within the range 73.9–117.1%, while for a 2% content it is in the range 61.7–108%. The lowest range of $R_c$ corresponds to a 3% content of nanosilver, and is 37.4–75.1%. However, these differences in attainable total draw values have only a small effect on the values obtained for the specific strength of the fibers. The highest values for specific strength, of up to 22.28 cN/tex, were recorded for fibers with a 1% content of nanosilver. For fibers containing 2% and 3% nanosilver the maximum strength value is ~21 cN/tex. Generally, the differences are small, of the order of 1.3 cN/tex. It is notable that fibers with different contents of silver nanoadditive

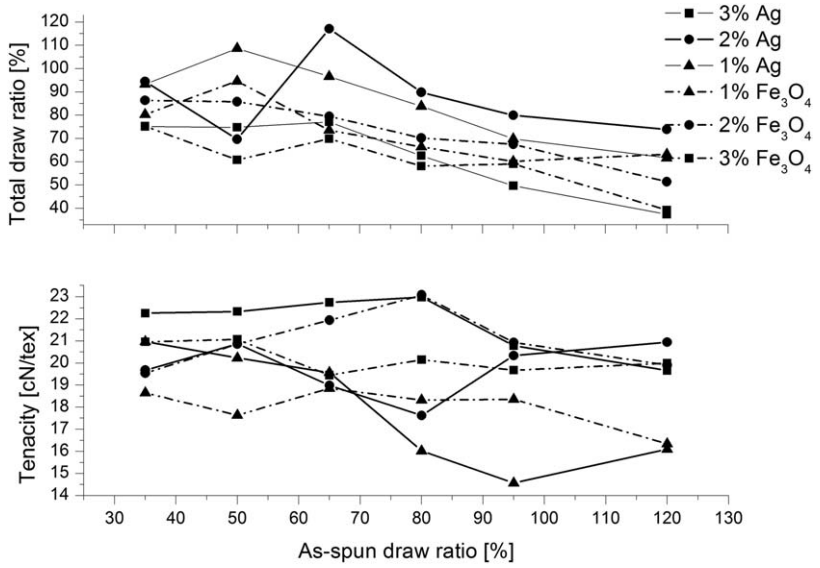


**Figure 4.** Relationship between total stretch and as-spun draw ratio, and specific strength and as-spun draw ratio, for fibers containing different quantities of nanosilver and nano $Fe_3O_4$.

achieve their maximum specific strength values at different values of the as-spun draw ratio (Figure 4).

The orientation of structural elements in the solidifying stream is a result of a lengthwise speed gradient (changing along the path of fiber formation), and the parameter, which controls the course of these processes is the as-spun draw ratio. Depending on the nature of the fiber structure produced at the solidification stage, there is also a difference in the deformability at the drawing stage. Both of these parameters and the relationship between them control the final orientation of structural elements and the specific strength of the final fibers. The strength of the final fibers is undoubtedly also affected by the presence in the solidifying stream of different quantities of metallic nanoadditives.

On the basis of the results obtained, it was concluded that fibers containing silver nanoadditive, formed at different as-spun draw ratios, have similar specific strength values. Increasing the quantity of nanoadditive probably hinders the process of connection between macromolecules, intensification of the network of such connections, gel syneresis, network contraction, and the creation of a homogeneous system. Its presence may also affect the course of phase transformations, and thus it may affect the nature of the gel formed and its deformability in further stages of the drawing process.

For fibers containing $Fe_3O_4$, similar dependences are found as for fibers with nanosilver. In this case, increasing the as-spun draw ratio leads to a reduction in the attainable total draw, while the deformability is lower as compared with fibers containing silver nanoadditive (Figure 4). For fibers containing 1% $Fe_3O_4$ the value is highest, with $R_c$ in the range 60.2–94.6%. For fibers containing 2% $Fe_3O_4$ the value of $R_c$ is from 51.4% to 86.4%. For those with 3% $Fe_3O_4$; however, the attainable total draw is in the range 39.3–75.3%. It is notable that the lowest and highest values of $R_c$ correspond to the extreme values of the as-spun draw ratio used. The slightly lower deformability during wet spinning process of fibers containing $Fe_3O_4$ may result from the larger dimensions of that nanoadditive. During solidification macromolecules are coming closer and are forming connections between them. The fibers are being solidified by formation chemical bonds by calcium. Introducing any additive to this network formation process cause interruption. Consequently, a slightly lower strength (by up to around 2 cN/tex) is recorded for fibers containing particular quantities of this nanoadditive as compared with fibers with silver nanoadditive (Figure 4).

Taking into account of the general tendency for the specific strength of fibers to decrease (or vary only to a small degree) as the as-spun draw ratio increases, for fibers containing silver nanoadditive in quantities of 1–3%, it can be assumed that it is favorable to carry out the forming process at an as-spun draw ratio of +50%. The strength of the fibers so formed varies over a narrow range of 20.2–22.3 cN/tex. However, for fibers containing $Fe_3O_4$ nanoadditive it is favorable to carry out the forming process with the as-spun draw ratio at the higher value of +80%.

It was found, based on our previous research in the case of fiber containing ceramic nanoadditives,[12,13] that the strength properties of the fibers decreases in function and the quantity of incorporated nanoadditives increases. Furthermore, in research on the fibers containing 2% of $Fe_3O_4$ nanoadditive this rule does not occur. The good strength properties of fibers with $Fe_3O_4$ may be explicated by the fact that the degree of crystallinity reaches the highest value. This compensates for the negative effect of the presence of nanoadditive on the fibers' strength properties.

The Young's modulus of calcium alginate fibers containing nanosilver and nano $Fe_3O_4$ lies within the fairly narrow range of 6.19–8.84 GPa, irrespective of the conditions of formation of the fibers and the nanoadditive content.

The elongation at rupture obtained for the nanocomposite fibers was 7.57% on average for fibers containing nanosilver, and 6.86% for fibers containing nano $Fe_3O_4$. Generally, the strength properties of both types of nanocomposite alginate fibers are suitable for their processing into nonwoven fabric by textile-making techniques. This applies above all to the elongation at rupture, which takes values of ~7%.

The strength properties of fibers are related not only to the orientation of structural elements in the direction of the axis of the fiber, but also to their crystalline structure—the degree of crystallinity and the sizes of crystallites. Analysis of the supramolecular structure of the two types of nanocomposite fibers was performed using the method of X-ray diffraction (WAXS). Analysis was made of the crystalline structure of fibers containing both types of nanoadditive in quantities of 1%, 2%, and 3%, formed with the as-spun draw ratio at +35%, +65%, and +120%. Also included in the analysis were fibers with 2% $Fe_3O_4$ nanoadditive formed at as-spun draw ratio of +80%. This selection was made on the ground that these were the fibers with the highest specific strength value, of the order of 23.07 cN/tex.

Analysis of the WAXS diffraction curves and calculation of the degree of crystallinity were performed using the WAXFIT computer program,[21,22] applying the methodology described in Ref. 12. Decomposition was carried out taking account of the complex structure of alginate macromolecules. These contain blocks of radicals of α-L-guluronic acid (G) and β-D-mannuronic acid, which form crystalline structures with different parameters. The elementary cell of polymannuronic acid has base edges **a** = 0.76 nm and **b** = 0.86 nm, and a height of **c** = 1.04 nm (in the direction of the chain of the macromolecule). For polyguluronic acid the corresponding parameters are **a** = 0.86 nm, **b** = 1.07 nm, and **c** = 0.87 nm. In fibers made from calcium alginate there therefore appear two types of crystalline regions—those of one type being formed from mannuronic blocks, and those of the other type from guluronic blocks. This is reflected in the form of the X-ray diffraction curves, which feature crystalline peaks corresponding to both types of crystallites. In the analysis of the diffraction curves, account was also taken of the effect of the calcium ions introduced into the fibers and located in the regions of "egg-box" junctions. These regions are formed between two guluronic blocks located in neighboring macromolecules. The pairs of guluronic blocks joined in this way, coming from neighboring macromolecules, form aggregates with a

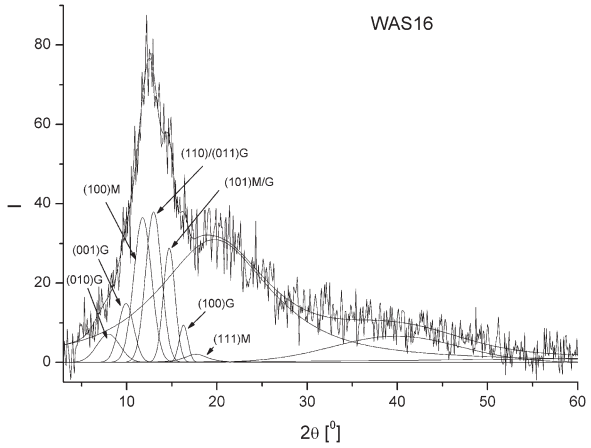


**Figure 5.** Diffractogram of sample WAS16 after subtraction of background, decomposed into crystalline peaks and amorphous components.

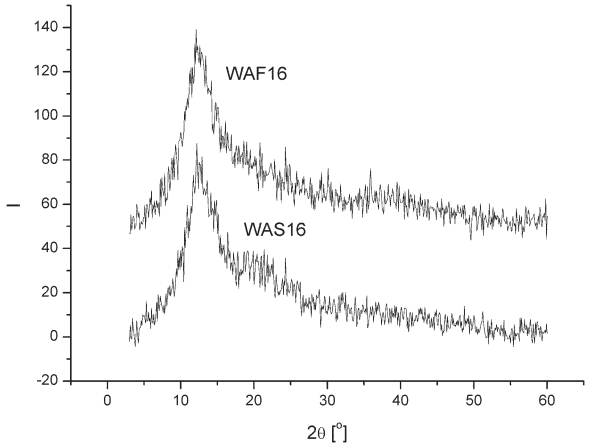


**Figure 6.** Diffractograms of samples WAF16 and WAS16

pseudo-hexagonal structure, in which the average distance between the macromolecule axes is $\mathbf{a} = 0.66$ nm. Associated with this parameter is a diffraction peak corresponding to the planes (100) of the hexagonal grid being distant from each other by $d_{100} = 0.57$ nm. On the diffractograms of the tested fibers (Figure 5), recorded at wavelength $\lambda = 0.154$ nm, this peak is found at an angle $2\theta = 15.5°$. Another effect resulting from the presence of calcium ions is the appearance of a peak coming from the family of planes (001), which in the case of "pure" guluronic acid is subject to systematic quenching.[23] On the diffractograms of the tested fibers, this peak appears at $2\theta = 10.3°$. The amorphous component was approximated using two wide maxima, one at a diffraction angle of $2\theta \approx 21°$, and the second at $2\theta \approx 40°$. Examples of diffractograms for both types of fibers are shown in Figure 6.

Crystallite dimensions were determined using Scherrer's formula, based on the half-widths of the three strongest peaks appearing on the diffractograms obtained for the fibers (Figure 6). The first of these comes from the family of grid planes (100) occurring in crystallites built of mannuronic blocks. The second results from the superposition of peaks originating from planes (110) and (011) in crystallites built from guluronic blocks. The third peak is a result of the superposition of two very closely positioned peaks originating from planes (101) in both types of crystallites.

The values determined for the degree of crystallinity of alginate fibers with both types of nanoadditive and the dimensions of the crystallites occurring in the fibers are given in Tables II and III.

As can be seen, the degree of crystallinity of both types of fibers is around 30%. This can be assumed to be caused by a significant quantity of regions of "egg-box" junctions forming in the fiber material because of the high concentration of calcium ions. The process of ordering and adoption of a mutually parallel orientation by pairs of macromolecules connected via such regions is much more difficult than in the case of single macromolecules. Consequently, the ability of the fiber material to crystallize is significantly reduced, and hence the degree of crystallinity decreases. It is nonetheless notable that the degree of crystallinity of fibers with $Fe_3O_4$ nanoadditive is greater than that of fibers with silver nanoadditive.

The dimensions of the crystallites in both types of fibers are similar, and lie in the range 3.7–6.1 nm; hence they are very

**Table II.** Degree of Crystallinity, Dimensions of Crystallites and Mechanical Properties of Fibers Containing Nanosilver

| Quantities of nanoadditives (%) | As-spun draw ratio (%) | Crystallinity (%) | $D_{100}$ (M) (nm) | $D_{110/011}$ (G) (nm) | $D_{101}$ (M/G) (nm) | Tenacity (cN/tex) |
|---|---|---|---|---|---|---|
| 3 | 35 | 31 | 3.9 | 5.1 | 5.3 | 20.97 ± 0.97 |
| 3 | 65 | 27 | 4.7 | 5.9 | 5.7 | 19.57 ± 0.78 |
| 3 | 120 | 28 | 4.8 | 5.4 | 6.0 | 16.10 ± 1.06 |
| 2 | 35 | 29 | 4.5 | 6.1 | 5.6 | 19.68 ± 0.76 |
| 2 | 65 | 31 | 4.2 | 4.1 | 4.6 | 18.99 ± 0.78 |
| 2 | 120 | 30 | 3.7 | 4.0 | 5.4 | 20.95 ± 1.28 |
| 1 | 35 | 30 | 3.9 | 4.8 | 4.3 | 22.26 ± 1.14 |
| 1 | 65 | 35 | 4.1 | 4.4 | 5.7 | 22.75 ± 1.80 |
| 1 | 120 | 31 | 4.1 | 4.6 | 5.3 | 19.66 ± 2.20 |

Data of crystallinity measurements are given with margin of observational error at level of 3%. Tenacity data are given with SD value. After every measurement value and "±" SD is given for each measurement.

**Table III.** Degree of Crystallinity, Dimensions of Crystallites and Mechanical Properties of Fibers Containing Nanomagnetite ($Fe_3O_4$)

| Quantities of nanoadditives (%) | As-spun draw ratio (%) | Crystallinity (%) | $D_{100}$ (M) (nm) | $D_{110/011}$ (G) (nm) | $D_{101}$ (M /G) (nm) | Tenacity (cN/tex) |
|---|---|---|---|---|---|---|
| 3 | 35 | 37 | 4.2 | 5.7 | 4.9 | 18.65 ± 1.07 |
| 3 | 65 | 34 | 4.7 | 4.6 | 4.5 | 18.85 ± 0.93 |
| 3 | 120 | 35 | 3.8 | 4.4 | 5.2 | 16.34 ± 1.10 |
| 2 | 35 | 32 | 4.8 | 4.9 | 5.6 | 19.54 ± 1.27 |
| 2 | 65 | 33 | 4.4 | 4.9 | 5.4 | 21.94 ± 1.05 |
| 2 | 80 | 37 | 4.1 | 5.5 | 4.5 | 23.07 ± 1.11 |
| 2 | 120 | 37 | 4.2 | 4.6 | 4.7 | 19.91 ± 1.30 |
| 1 | 35 | 34 | 4.7 | 5.8 | 4.8 | 20.96 ± 1.09 |
| 1 | 65 | 32 | 4.4 | 5.1 | 5.1 | 19.45 ± 0.90 |
| 1 | 120 | 31 | 4.4 | 5.4 | 5.8 | 19.99 ± 1.34 |

small crystallites. There is no clear correlation between the sizes of crystallites and the conditions of fiber formation. The differences found between the sizes of guluronic and mannuronic crystallites are within the range of measurement error, which in view of the significant overlapping of peaks (see Figure 5) is of the order of 1 nm.

In the case of fibers containing nanosilver, it can be noted that the results of the measurements of degree of crystallinity are fairly well correlated with the strength parameters. Namely, the fibers with the highest strength and Young's modulus has the highest degree of crystallinity. This relationship also holds within each of the three groups of fibers, those containing 1%, 2%, and 3% nanosilver, respectively. At the same time, an increase in the concentration of nanosilver in the fiber is associated with a decrease in the strength and in the degree of crystallinity. Most probably, the presence of grains of nanosilver in the solidifying stream constitutes a significant structural defect and a significant obstacle to the process whereby chains of macromolecules adopt a configuration enabling the formation of crystallites from guluronic and mannuronic blocks. No relationship was found; however, between the degree of crystallinity and the as-spun draw ratio. However, in the case of calcium alginate fibers containing ceramic nanoadditives, variation (over a similar range) in the as-spun draw ratio towards larger positive values was found to lead to an increase in the degree of crystallinity by ~4–5%. The dimensions of the crystallites in calcium alginate fibers containing 3% nanosilver (which are those with the lowest degree of crystallinity) are markedly greater than those in the fibers with the remaining two values of nanoadditive content.

### Analysis of the Sorption Properties of Nanocomposite Alginate fibers with Regard to Their Porous Structure

Analysis of the sorption properties of fibers containing nanosilver and nano $Fe_3O_4$ shows that these properties are strongly controlled by the hydrophilic nature of the material. Moisture sorption at 65% RH is around 20%, and at 100% RH it reaches 35–40%, while the value for water retention is ~90%. Neither the quantity nor the type of nanoadditive causes significant changes in the sorption properties of the fibers. Moisture sorption at 65% and 100% RH and water retention are shown as functions of the as-spun draw ratio, for different values of nanoadditive content, for (by way of an example) the fibers containing nanosilver (Figure 7). It can be observed that changes in the as-spun draw ratio also do not cause changes in the fibers' moisture sorption and water retention properties.

Changes in the quantity of nanoadditives introduced into the fiber material, as well as changes in the as-spun draw ratio, also do not cause changes in the nature of the porous structure of the fibers. Figures 8 and 9 show curves of pore distribution as a

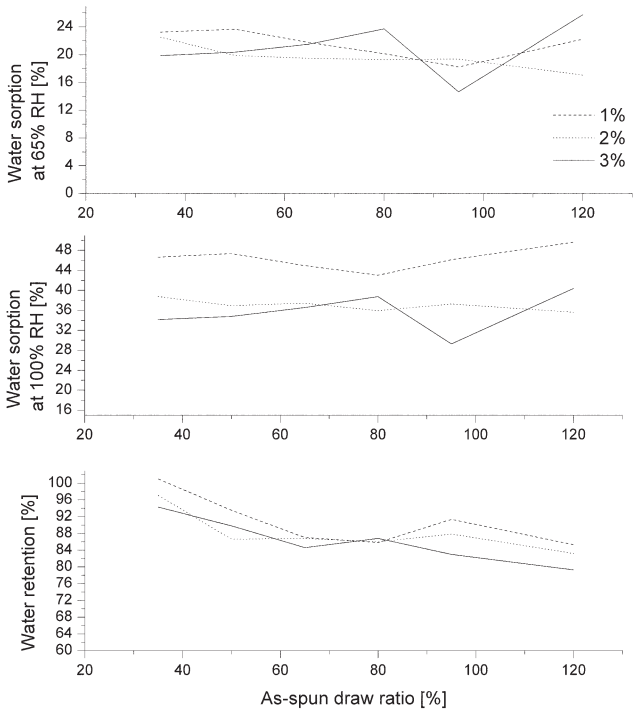


**Figure 7.** Moisture sorption at 65% and 100% RH and water retention, as functions of the as-spun draw ratio, for fibers containing different quantities of silver nanoadditive.

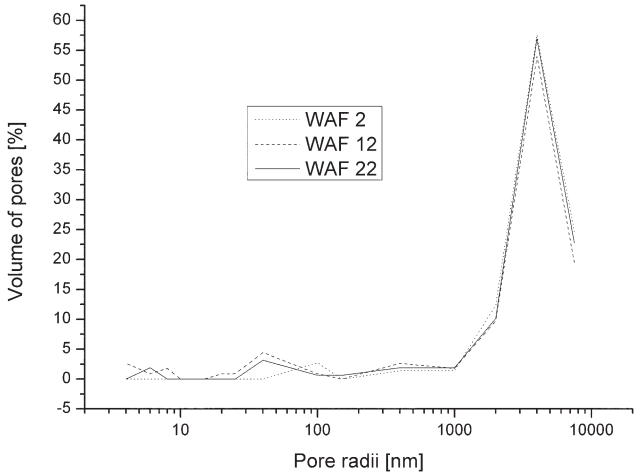


**Figure 8.** Curves of pore distribution as a function of pore radius, for fibers containing different quantities of $Fe_3O_4$ nanoadditive, formed at a draw ratio of +65%.

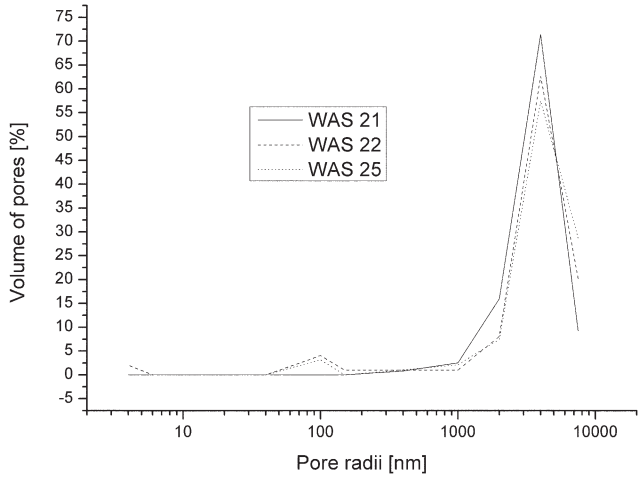


**Figure 9.** Curves of pore distribution as a function of pore radius, for fibers containing 1% silver nanoadditive, formed at different draw ratios.

function of pore radius, for (by way of an example) fibers containing different quantities of $Fe_3O_4$ nanoadditive formed at as-spun draw ratio of +65%, and for fibers containing 1% nano-silver formed at different draw ratios.

### Analysis of the Cross-Sectional Shape and the Surface of the Fibers

Another element of the macroscopic structure of fibers, which affects their sorption and strength properties is the shape of the cross-section and of the edge line. In the wet spinning method

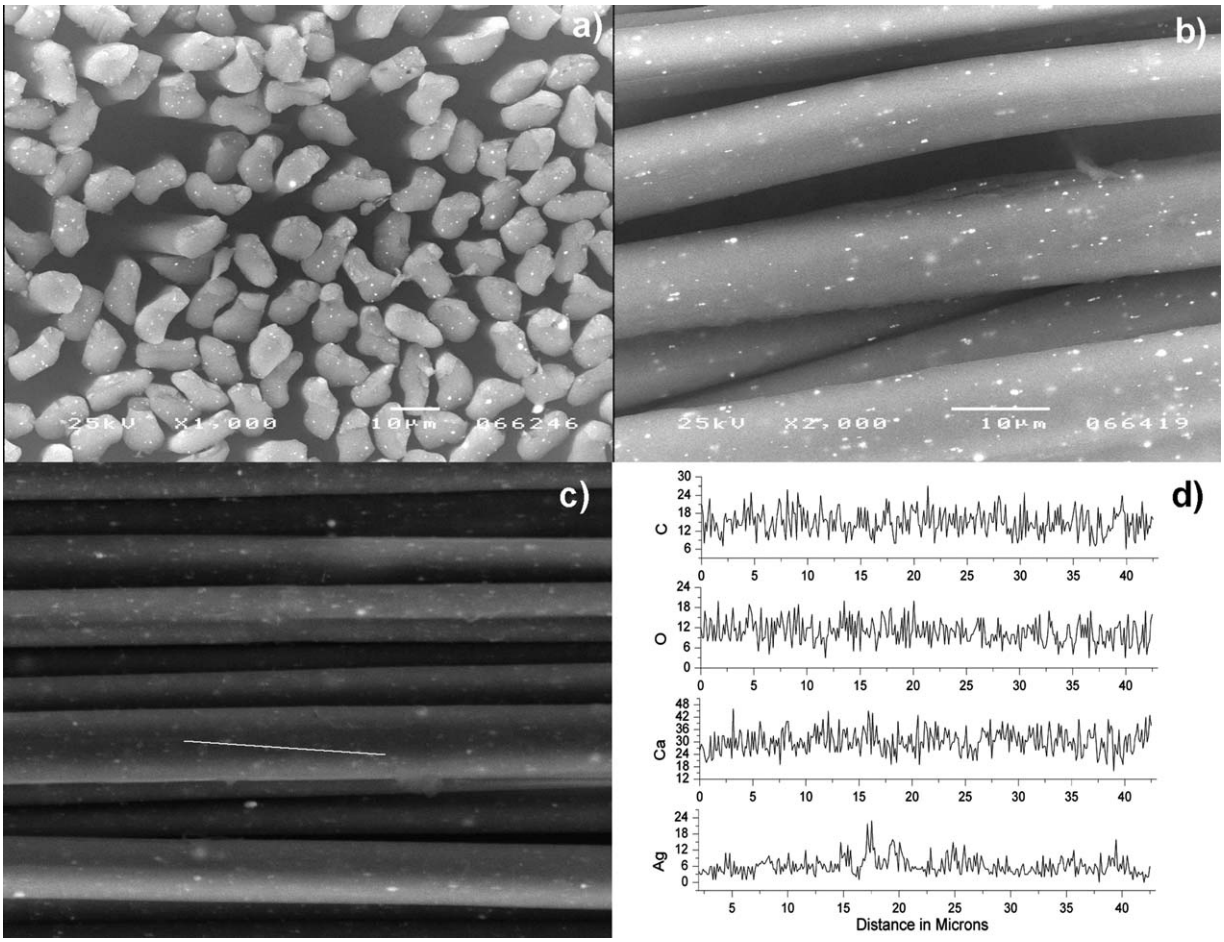


**Figure 10.** (a) Cross-sections and (b) lengthwise views of fibers containing 1% silver nanoadditive (sample WAS 24) and (c and d) results of X-ray microanalysis performed along the marked line of fibers containing 3% silver.

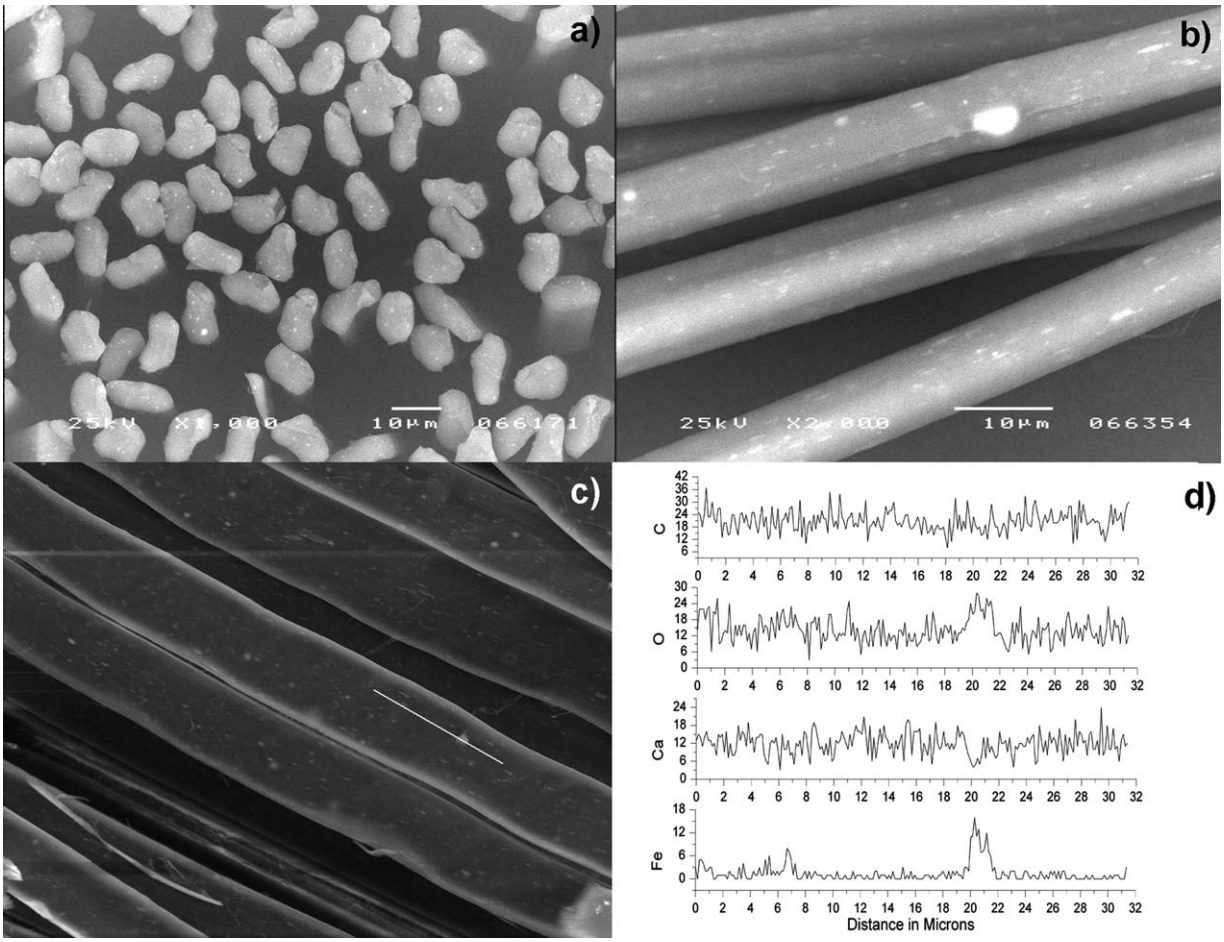


**Figure 11.** (a) Cross-sections and (b) lengthwise views of fibers containing 2% $Fe_3O_4$ nanoadditive (sample WAF 14) and (c and d) results of X-ray microanalysis performed along the marked line of fibers containing 3% $Fe_3O_4$.

of fiber formation, when the solidification process is controlled by processes of mass exchange, both of these factors depend on the ratio between the streams of solvent and nonsolvent.[24] However, in the case of alginate fibers, the solidification process is controlled by chemical reactions, and an important part is played by the syneresis of the formed gel, where solvent is "squeezed" out of the walls. Analysis of the effect of the as-spun draw ratio on the shape of the cross-section of calcium alginate fibers containing ceramic nanoadditives has shown[10,12,13,16] that an increase in this ratio is accompanied by a flattening of the cross-sectional shape. Fibers containing the metallic nanoadditives silver and $Fe_3O_4$, formed at as-spun draw ratio of +80%, also display this type of flattened cross-sectional shape (Figures 10 and 11). Also visible is the presence of both types of nanoadditive dispersed in the material. They occur sporadically in the form of clusters, in spite of the application of a sonication process. The presence of nanoadditives is also clearly visible on the surface of the fibers (Figures 10 and 11), and their even dispersion was confirmed by the SEM + EDS method (Figures 10 and 11). The presence of larger peaks on the spectra corresponding to the elements silver or iron indicates the occurrence of agglomerations of the nanoadditives.

## CONCLUSIONS

Irrespective of the quantity and type of nanoadditive (silver or $Fe_3O_4$) introduced, aqueous solutions of sodium alginate are shear thinning non-Newtonian fluids without flow boundary. Solutions containing silver as a nanoadditive are slightly closer to Newtonian than those with $Fe_3O_4$.

The strength properties of calcium alginate fibers containing nanosilver in quantities from 1% to 3% are correlated with their degree of crystallinity. Fibers containing $Fe_3O_4$ nanoadditive, however, have a higher degree of crystallinity in combination with lower strength properties. An exception is fibers containing 2% $Fe_3O_4$ formed at as-spun draw ratio of +80%, which have both the highest specific strength and the highest degree of crystallinity.

The sorption properties of alginate fibers containing nanosilver or nano $Fe_3O_4$ are determined by the hydrophilic nature of the material. These properties are negligibly affected by the macroscopic structure of the fibers, which is dependent to a small degree on the conditions of fiber formation. High water retention values may result from an ability to bind water in the form of polymorphous clusters by way of unsubstituted OH groups in the fiber material or located on the fiber surface.

The simultaneous SEM and EDS analysis indicated the presence of the nanoadditives both on the surface of the fibers and throughout the whole of their mass. This may bring about an increase in the effectiveness of the action of each of the studied metallic nanoadditives.

## ACKNOWLEDGMENTS

The research presented in the article was financed by The National Centre for Research and Development, project No. NR08-0032-10.

## REFERENCES

1. Rutner, B. D.; Hoffman, A. S.; Schoen, F. J.; Lemons, J. E. Biomaterials Science. As Introduction to Materials in Medicine. Elsevier: London, **2004**.
2. Hosler, J. A. *US Pat. 6*,153,214 (**2000**).
3. Qin, Y.; Gilding, D. K. *US Pat. 6*,080,420 (**2000**).
4. Hench, L. L.; Jones, J. R. Biomaterials, Artificial Organs and Tissue Engineering. Woodhead Publishing: Cambridge, **2005**.
5. Hashimoto, T.; Suzuki, Y.; Tanihara, M.; Kakimaru, Y.; Suzuki, K. *Biomaterials* **2004**, *25*, 1407.
6. Skjåk-Bræk, G.; Larsen, B.; Grasdalen, H. *Carbohydr. Res.* **1986**, *154*, 239.
7. Martinsen, A.; Skjåk-Bræk, G.; Smidsrød, O.; Zanetti, F.; Paoletti, S. *Carbohydr. Polym.* **1991**, *15*, 171.
8. Mikołajczyk, T.; Wołowska-Czapnik, D. *Fibres Text. East. Eur.* **2005**, *3*, 13.
9. Mikołajczyk, T.; Urbaniak–Domagała, W.; Wołowska-Czapnik, D. *J. Appl. Polym. Sci.* **2006**, *101*, 686.
10. Boguń, M.; Stodolak, E.; Menaszek, E.; Ścisłowska-Czarnecka, A. *Fibres Text. East. Eur.* **2011**, *19*, 17.
11. Boguń, M.; Łącz, A. *J. Therm. Anal. Calorim.* **2011**, *106*, 953.
12. Boguń, M.; Rabiej, S. *Polym. Compos.* **2010**, *31*, 1321.
13. Boguń, M. *Fibres Text. East. Eur.* **2010**, *4*, 11.
14. Stodolak, E.; Paluszkiewicz, C.; Boguń, M.; Błażewicz, M. *J. Mol. Struct.* **2009**, *924*, 208.
15. Boguń, M.; Mikołajczyk, T.; Rabiej, S. *J. Appl. Polym. Sci.* **2009**, *114*, 70.
16. Mikołajczyk, T.; Wołowska-Czapnik, D.; Boguń, M. *J. Appl. Polym. Sci.* **2008**, *107*, 1670.
17. Chalupka, K.; Malam, Y.; Seifalian, A. M. *Trends Biotechnol.*, **2010**, *28*, 580.
18. Faunce, T.; Watal, A. *Nanomedicine* **2010**, *5*, 617.
19. Kumar, P. T. S.; Abhilash, S.; Manzoor, K.; Nair, S. V.; Tamura, H.; Jayakumar, R. *Carbohydr. Polym.* **2010**, *80*, 761.
20. Boguń, M. *Fibres Text. East. Eur.* **2009**, *5*, 17.
21. Rabiej, M. *Fibres Text. East. Eur.* **2003**, *11*, 83.
22. Rabiej, M.; Rabiej, S. Analiza rentgenowskich krzywych dyfrakcyjnych polimerów za pomocą programu komputerowego WAXFIT. Publishing House ATH: Bielsko-Biała, **2006**.
23. Sikorski, P.; Frode, M.; Skjak-Bræk, G.; Stokke, B. T. *Biomacromolecules* **2007**, *8*, 2098.
24. Ziabicki, A. Fundamentals of Fibre Formation: The Science of Fibre Spinning and Drawing. Wiley: London, **1976**.